

Supporting Information

Two-dimensional arrays of hexagonal plasmonic necklaces for enhanced SHG

Alejandro Gómez-Tornero, Christos Tserkezis, Luis Mateos, Luisa E. Bausá and Mariola O Ramírez*

1. Calculated extinction spectra of hexagonal plasmonic necklaces

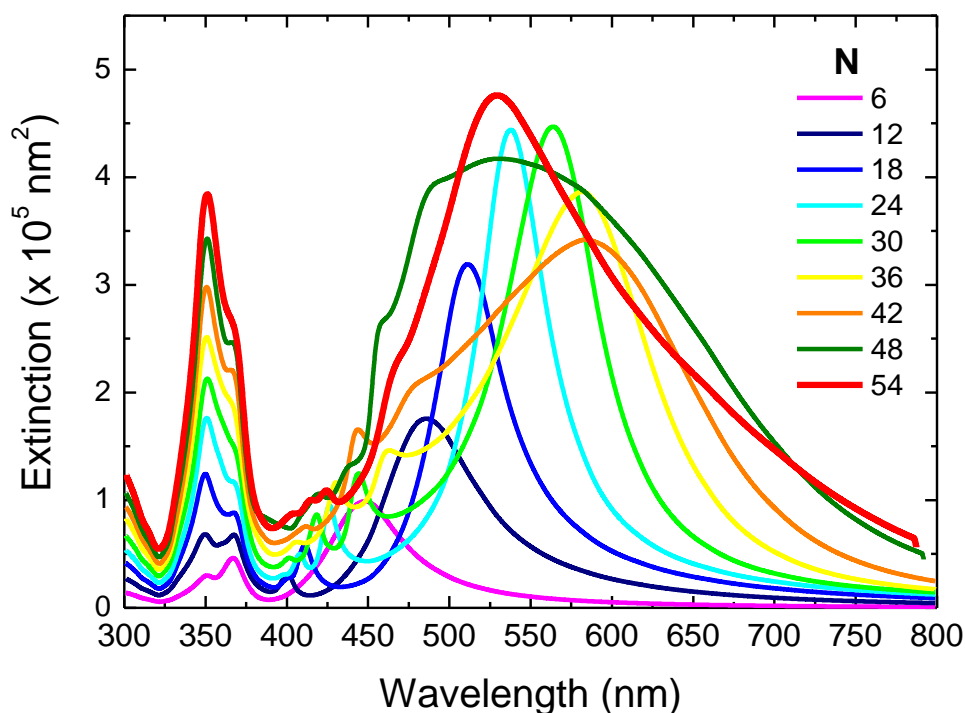


Figure S1: Extinction cross section spectra of hexagonal plasmonic necklaces containing different number, N , of 50-nm Ag nanoparticles separated by 2-nm gaps, in air, illuminated by a plane wave polarised along one of the hexagon sides.

Figure S1 shows a series of simulations for perfect hexagons of 50-nm Ag NPs separated by 2-nm gaps, in air, illuminated by a plane wave polarised along one of the hexagon sides. In agreement with the experiments, the simulations show that the spectral response of a hexagon is dominated by a broad, long-wavelength plasmonic mode associated with the collective excitation of the nanoparticles (NPs) forming the necklace. As we increase the necklace size, this mode broadens and shifts to longer wavelengths until it eventually stop red shifting for hexagons of about 36 NPs. Increasing the number of interacting NPs above this number results into a further spectral broadening of the resonance because of its overlap

with higher-order modes - which continue red-shifting even after the 1st order mode has saturated with hexagon size. A convergence of the position of the main mode at around 530 nm is obtained for hexagons containing about 54 NPs (10 NPs side).

2. Polarized SHG images of bare hexagonal ferroelectric domains in LiNbO₃

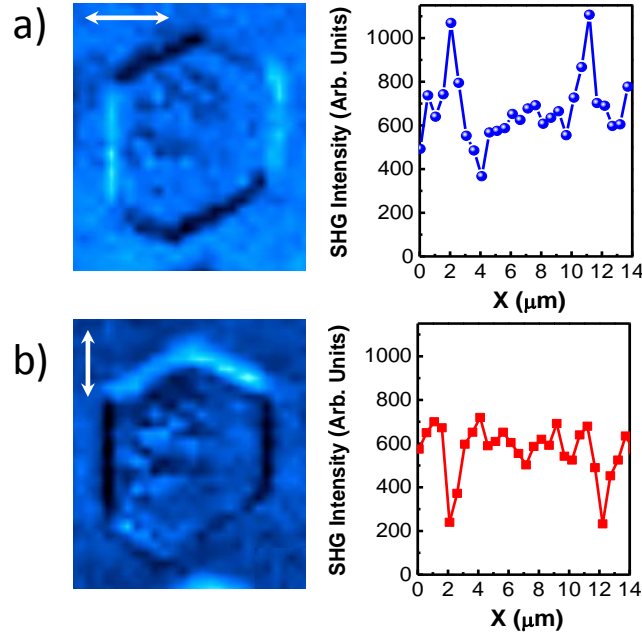


Figure S2: (a,b) SHG microscopy images of a single hexagonal domain in LiNbO₃ for different polarization configurations. The arrows indicate the polarization state of the fundamental beam with respect to the orientation of the hexagon. The associated SHG intensity profiles were obtained by integrating the SHG signal across the horizontal dimension of the hexagon.

Figure S2 shows the spatial distribution of the integrated SHG obtained for a single hexagonal domain in the absence of metallic nanoparticles (bare substrate). The images were obtained by carefully focussing the fundamental laser beam on the crystal surface. The incident pump power was 10 mW. As seen, the spatial distribution of the integrated SHG at the domain wall surfaces in hexagonal domains depends on the polarization direction of the waves participating in the process. More specifically, when the fundamental beam is polarized parallel to the domain walls (red dots in the SH intensity profile), the monitored SHG at the boundaries decreases approximately by 50% and appears as dark lines on the homogeneous intensity background. In contrast, when the incident polarization is perpendicular to the wall, a brighter signal (about 2-3 times) is observed (blue dots in the SHG profiles). These results can be accounted for in terms of the destructive interference between the SHG signal arising from opposite domains and the effect of symmetry breaking at the walls,^[1,2] which strongly

affects the condition for SHG at those regions.^[3-7]. Our results evidence that the SHG processes at domain walls in LiNbO₃ occurs for the two different polarization configuration analyzed in this work (orthogonal polarizations states), showing a more efficient behavior when the light fields oscillate perpendicular to them.

3. Comparison of the SHG response from LiNbO₃ (bare substrate) and the hybrid plasmonic-nonlinear structures (Necklaces/LiNbO₃)

Table SI summarizes the SHG results obtained for the three cases of interest, *i.e* single domain region far away from domain walls (LNB), ferroelectric domain walls in the absence of metallic nanostructures (LNB +DW) and domain wall surfaces on which strongly coupled Ag nanoparticles were deposited (LNB+DW+NPs).

For a proper estimation, the measured SHG signal has been normalized by the square of the incident intensity: $I_{2\omega}/(I_{\omega})^2$. To avoid damaging the structures, the SHG experiments in the hybrid plasmonic/LNB system were performed with an incidental pump power of ~1 mW. In the case of the bare substrate, due to the strong enhancement provided by the metallic nanoparticles on the domain walls, and to make possible the comparison, the incident pump power had to be increased up to 10 mW (Figure S2).

TABLE SI: Normalized SHG intensity for different polarization configurations of the fundamental beam with respect to the domain walls.

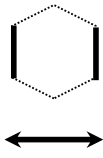
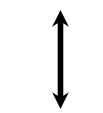
Polarization Configurations	<i>Normalized SHG Intensity Counts (Arb. Units)</i>		
	LNB	LNB+DW	LNB+DW+NP
	600 (500-700)	1100 (900-1200)	---
	600 (500-700)	250 (200-300)	2500 x 10 ² (1500-3500) x 10 ²

Table SI: Normalized SHG intensity measured on single domain regions (LNB), ferroelectric domain walls in the absence of metallic nanostructures (LNB +DW) and domain wall surfaces with Ag nanoparticles (LNB+DW+NPs). The arrows indicate the polarization state of the fundamental beam with respect to the orientation of the hexagonal domains. Red numbers correspond to average values. Minimum and maximum measured values are shown in brackets.

References:

- [1] E. A. Eliseev, A. N. Morozovska, S. V. Kalinin, Y. Li, J. Shen, M. D. Glinchuk, L.-Q. Chen, V. Gopalan, *J. Appl. Phys.* **2009**, *106*, 084102.
- [2] V. R. Aravind, A. N. Morozovska, S. Bhattacharyya, D. Lee, S. Jesse, I. Grinberg, Y. L. Li, S. Choudhury, P. Wu, K. Seal, A. M. Rappe, *Phys. Rev. B* **2010**, *82*, 024111.
- [3] S. A. Denev, T. T. A. Lummen, E. Barnes, A. Kumar, V. Gopalan, *J. Am. Ceram. Soc.* **2011**, *94*, 2699.
- [4] M. Flörshemer, R. Paschotta, U. Kubitscheck, Ch. Brillert, D. Hofmann, L. Heuer, G. Schreiber, C. Verbeek, W. Sohler, H. Fuchs, *Appl. Phys. B* **1998**, *67*, 593.
- [5] S. I. Bozhevolnyi, J. M. Hvam, K. Pedersen, F. Laurell, H. Karlsson, T. Skettrup, M. Belmonte, *Appl. Phys. Lett.* **1998**, *73*, 1814.
- [6] A. Fragemann, V. Pasiskevicius, F. Laurell, *Appl. Phys. Lett.* **2004**, *85*, 375.
- [7] S. I. Bozhevolnyi, K. Pedersen, T. Skettrup, X- Zhang, M. Belmonte, *Opt. Comm.* **1998**, *152*, 221.